DYNAMIC MODELING AND CONTROL OF ELASTIC BEAM FIXED ON A MOVING CART AND CARRYING LUMPED TIP MASS

Fadi A. Ghaith, *fadiag@kfupm.edu.sa* Department of Mechanical Engineering, King Fahd University of Petroleum and Minerals, Dhahran, Saudi Arabia.

Mohammad N. Hamdan, *mnader@ju.edu.jo* Department of Mechanical Engineering ,University of Jordan, Amman, Jordan.

ABSTRACT

In this paper, a Bernoulli – Euler beam fixed on a moving cart and carrying a lumped tip mass is considered. The equations of motion which describe the global motion as well as the vibrational motion were derived using the extended Hamilton's principle. The obtained equations of motion are analyzed by means of the unconstrained modal analysis. In order to eliminate the need of sensor placement at the tip of the cantilever beam, as most of the practical control implementations require that sensors and actuators to be placed in accessible locations, the Linear Quadratic Estimator (LQE) approach was utilized to estimate the vibrations of any point on the span of the elastic cantilever beam in the presence of process and measurement noises. For the purpose of suppressing the vibrations at the tip of the beam, an active optimal controller was designed based on the Linear Quadratic Gaussian (LQG) method. Numerical simulation results demonstrated the capability of the developed optimal controller in eliminating the vibrations at the tip of the beam as well as to improve the positioning accuracy.

Keywords: Unconstrained modal analysis, Linear quadratic estimator, Linear quadratic Gaussian.

1. INTRODUCTION

The beam is considered as one of the fundamental elements of an engineering structure. It finds use in varied structural applications. Moreover, structures like forklift vehicles or ladder cars that carry heavy loads, military airplane wings with storage loads on their span and antenna operated in the space can be modeled as a flexible beam carrying a concentrated mass and being fixed on a moving cart. Due to the presence of vibration in such systems, it leads to undesirable effects such as structural and mechanical failures, though vibration suppression has been main requirement for their design and safe operation. Active control falls among the most feasible techniques for vibration suppression in axially moving structures, where passive techniques may become ineffective or impractical. On the other side, unconstrained modal analysis is considered as a powerful tool to generate accurate mode shapes of the system, such analysis may provide useful information which may enhance the design of the optimal controller. Many studies were reported in the literature concerned of the mathematical modeling of similar systems based on the linear formulation. Exact frequency equation of a uniform cantilever beam carrying a slender tip mass whose center of gravity didn't coincide with the attachment point has been developed by [Bhat and Wanger, 1979]. [To, 1982] calculated the natural frequencies and mode shapes of a mast antenna structure, but he modeled it as a cantilever beam with base excitation and tip mass because the total mass of the beam-mass system is negligible compared with that to the base. [Park et al., 1998] obtained the linear equations of motion, frequency equations and exact solutions of the motion of flexible beam fixed on a moving cart and carrying a lumped tip mass using unconstrained modal analysis. [Park et al., 2000] considered a Bernoulli-Euler beam fixed on a moving cart and carrying a concentrated mass attached at an arbitrary position along the beam, and the linear equations of motion which describe the global motion as well as vibrations motion were derived. Vibration suppression has been a requirement for the design and operations in many engineering structures. Due to the development in the area of control systems, active controllers have been implemented in several vibration suppression applications. [Khulief, 2000] has proposed the control of a rotating beam mounted on a rigid hub using linear quadratic regulator. [Zimmerman and Cudeney, 1989], [Yousfi-Koma and Vukovich, 2000], [Mallory and Miller, 2000], [Lee and Eillott, 2001], all have also suggested placing sensors at various locations along the span of the beam for monitoring and control purposes. [Sinawi and Hamdan, 2003] developed a new approach for estimating the vibration of any point on the span of a rotating flexible beam mounted on a compliant hub (plant) in the presence of process and measurements noise based on the Linear Quadratic Estimator (LQE) technique. At this point one can conclude that an active control law that uses a consistent dynamic model and utilizes the linear quadratic regulator in absence of process and measurement noise is not fully addressed, in particular when unconstrained modal analysis is utilized as the modeling tool. In this paper, the equations of motion of a Bernoulli-Euler cantilever beam clamped on a moving cart and carrying lumped mass are analyzed by means of the unconstrained modal analysis, and a unified characteristic equation for calculating the natural frequencies of the system. The natural frequencies obtained from the unconstrained modal analysis are used to develop an active modal controller based on Kalman filter estimator and linear quadratic regulator in order to reduce the end vibration as well as to improve the positioning accuracy.

2. MODEL FORMULATION

The equations of motion of a Bernoulli-Euler cantilever beam clamped on a moving cart and carrying lumped mass on its tip are derived using the extended Hamilton's principle. It should be recognized that the addressed dynamic model is considered to be linear by neglecting the effect of axial shortening.

2.1 System Description and Assumptions

Consider the planar motion of the beam-mass-cart system, shown in Fig.1. The elastic beam is assumed to follow the Bernoulli-Euler beam model and to be clamped tightly on the moving cart. In deriving the equations of motion, it is assumed that the beam material is linearly elastic and undergoes small deformation.

2.2 Equations of Motion

The equations of motion and the boundary conditions of the beam-mass-cart system are derived using the extended Hamilton's principle. Defining the variation of the functional *I*, which represents the integrand of the Lagrangian function *L* over the initial and final time instants, t_o and t_f respectively, and considering the fact that the variation and integral operators commute, we can write for the actual path that:

$$\int_{t_o}^{t_f} \left(\delta L + \delta W_{nc}\right) dt = 0 \tag{1}$$

where δW_{nc} denotes the work done by non-conservative forces such as external forces and moments.

Referring to the Cartesian coordinates shown in Fig. 1, the beam potential and kinetic energy are given by equations (2) and (3) respectively,

$$V = \frac{EI}{2} \int_0^l (u'')^2 \, dy \tag{2}$$

$$T = \frac{1}{2}\, \mathrm{M}\dot{\mathrm{x}}^2 + \frac{1}{2} \int_0^l \rho_o \left(\dot{x} + \dot{u}\right)^2 dy + \frac{1}{2} m \delta(y - l)\left(\dot{x} + \dot{u}\right)^2 \tag{3}$$

where

M: mass of the cart.

m: lumped mass at the tip of the beam .

ρ_o: mass per unit length of the beam .

l: length of the beam .

u(y,t) : lateral deformation of the beam at a distance *y* measured from the fixed end of the beam along the neutral axis in the undeformed configuration and at time *t* .

EI: The flexural stiffness of the beam.

δ(y-l): The dirac δ-function.

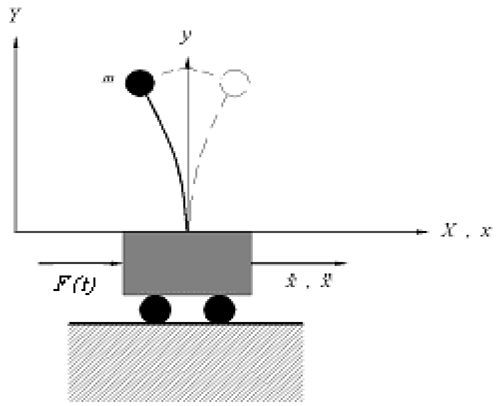

Fig. 1: Schematic of the beam-mass-cart system.

Substituting equations (2) and (3) into equation (1), noting that $L = T - V$, and after some mathematical manipulations including integration by parts, yields

$$M\,\ddot{x} + \int_0^l \left[\rho_o + m\delta(y-l)\right]\left(\ddot{x} + \ddot{u}\right)dy = F(t) \tag{4}$$

$$EI\,u'''' + \left[\rho_o + m\delta(y-l)\right](\ddot{x} + \ddot{u}) = 0 \tag{5}$$

$$u(0,t) = 0, u'(0,t) = 0, EI\,u''(l,t) = 0, EI\,u'''(l,t) = 0 \tag{6}$$

3. MODAL ANALYSIS

In this study, the obtained equations of motion are analyzed utilizing the unconstrained modal analysis which admits the presence of the external forcing terms. Assuming that the position of the cart *x(t)* has a solution of the form:

$$x(t) = \alpha(t) + \beta\,q(t) \tag{7}$$

where *α(t)* describes the motion of the center of mass . Therefore, the motion of the center of the mass without perturbation can be expressed as:

$$M_t\ddot{\alpha}(t) = F(t) \tag{8}$$

where M_t is the total mass of the beam-mass-cart system such $M_t = M + m + m_b$ and m_b represents the mass of the flexible beam such $m_b = \rho_o\,l$.

Also, the deflection of the beam *u(y,t)* is assumed to have the solution of the form

$$u(y,t) = \Phi(y)q(t) \tag{9}$$

Defining $\psi(y) = \beta + \Phi(y)$, and substituting equations (7) and (9) into equation (5), one obtains

$$EI\psi''''(y)\,q(t) + \left[\rho_o + m\delta(y-l)\right]\left[\psi(y)\,\ddot{q}(t) + \ddot{\alpha}(t)\right] = 0 \tag{10}$$

To get the normal mode solutions, where the effect of the external forces vanishes, one can decompose equation (10) into the following two ordinary differential equations using the principle of separation of variables

$$\ddot{q}(t)+\omega^2 q(t)=0 \tag{11}$$

$$EI\psi''''(y)-\omega^2\left[\rho_o+m\delta(y-l)\right]\psi(y)=0 \tag{12}$$

where ω is the natural frequency of the beam-mass-cart system. Hence, the boundary conditions defined by equation (6) can be rewritten as

$$\psi(0)=\beta,\psi'(0)=0,\ \psi''(l)=0,\psi'''(l)=0 \tag{13}$$

Solving equation (12) using Laplace transforms, and after several mathematical manipulations, one can obtain the solution of $\psi(y)$ as

$$\begin{aligned}\psi(y)&=\frac{\beta}{2}(\cos ky+\cosh ky)-\frac{\psi''(0)}{2k^2}(\cos ky-\cosh ky)-\frac{\psi'''(0)}{2k^3}(\sin ky-\sinh ky)\\&-\frac{m\omega^2\psi(l)}{2EIk^3}U(y-l)\left[\sin k(y-l)-\sinh k(y-l)\right]\end{aligned} \tag{14}$$

where $U(y-l)$ is a unit step function at $y=l$, and k represents the modal frequency and can be expressed as $k^4=\frac{\rho_o\omega^2}{EI}$ .The constants $\psi''(0)$ and $\psi'''(0)$ can be obtained from the last two boundary conditions given by equation (13) as follow

$$\psi''(0)=\frac{m\omega^2\psi(l)}{2EIk}\frac{1}{1+\cos kl\cosh kl}\left\{2(\sin kl+\sinh kl)\right\}+\beta k^2\frac{\sin kl\sinh kl}{1+\cos kl\cosh kl} \tag{15}$$

and

$$\psi'''(0)=-\frac{m\omega^2\psi(l)}{2EI}\frac{1}{1+\cos kl\cosh kl}\left\{2(\cos kl+\cosh kl)\right\}-\beta k^3\frac{\cos kl\sinh kl+\sin kl\cosh kl}{1+\cos kl\cosh kl} \tag{16}$$

Thus, from equations (15) and (16) , $\psi(y)$ can be expressed as

$$\psi(y)=A(y)\psi(l)+B(y)\beta \tag{17}$$

where

$$A(y)=\frac{m\omega^2}{4EIk^3}\left\{\begin{array}{l}\frac{\cos ky-\cosh ky}{1+\cos kl\cosh kl}\left[-2(\sin kl+\sinh kl)\right]\\+\frac{\sin ky-\sinh ky}{1+\cos kl\cosh kl}\left[2(\cos kl+\cosh kl\right]\\-2U(y-l)\left[\sin k(y-l)-\sinh k(y-l)\right]\end{array}\right\} \tag{18}$$

and

$$B(y)=\frac{1}{2}\begin{bmatrix}\cos ky+\cosh ky-\dfrac{\sin kl\sinh kl}{1+\cos kl\cosh kl}(\cos ky-\cosh ky)\\ +\dfrac{\cos kL\sinh kL+\sin kl\cosh kl}{1+\cos kl\cosh kl}(\sin ky-\sinh ky)\end{bmatrix}\tag{19}$$

Integration of equation (5) with respect to y and substituting equation (4) into the resulting equation gives

$$M\,\ddot{x}+EI\,u'''(0,t)=F(t)\tag{20}$$

When *F(t)* is assigned to be zero, and among substituting equations (7) , (8) and (11) into equation (20) yields

$$\beta=\frac{EI}{M\omega^2}\Phi'''(0)=\frac{EI}{M\omega^2}\psi'''(0)\tag{21}$$

Utilizing equations (16) and (21), β can be found as

$$\beta=\frac{C\psi(l)}{1-D}\tag{22}$$

where

$$C=\frac{-m}{2M}\frac{1}{1+\cos kl\cosh kl}\{2(\cos kl+\cosh kl)\}\qquad and \qquad D=-\frac{\rho_o}{Mk}\frac{\sin kl\cosh kl+\cos kl\sin kl}{1+\cos kl\cosh kl}$$

Finally, equations (17) and (22) lead to

$$\psi(y)=\left[A(y)+\frac{C}{1-D}B(y)\right]\psi(l)=F(y)\psi(l)\tag{23}$$

3.1 The Frequency Equation

Equation (23), at $y=l$, gives the following equation:

$$[1-D-A(l)+A(l)D-B(l)C]\psi(l)=0\tag{24}$$

As $\psi(l)=0$ yields a trivial solution, the inner part of the bracket in equation (24) must vanish. From this condition, and after some mathematical manipulations, the frequency equation can be obtained as follows

$$\begin{aligned}&1+\cos\xi\cosh\xi+2r_1\cos\xi\cosh\xi+\frac{r_2}{\xi}(\cos\xi\sinh\xi+\sin\xi\cosh\xi)\\&+r_3\xi(\cos\xi\sinh\xi-\sin\xi\cosh\xi)=0\end{aligned}\tag{25}$$

where $r_1=\dfrac{m}{M}$, $r_2=\dfrac{m_b}{M}$, $r_3=\dfrac{m}{m_b}$ *and* $\xi=kl.$

3.2 Beam Deflections

If a function $\rho(y)$ is defined as

$$\rho(y) = \rho_o + m\,\delta(y - l) \tag{26}$$

Substituting equations (12) and (26) into equation (10), multiplying both sides of the resulting equation by $\Phi_j(y)$ and integrating over the problem domain, leads to

$$\sum_{i=1}^{\infty}\left[\ddot{q}_i(t) + \omega_i^2 q_i(t)\right]\int_0^l \rho(y)\psi_i(y)\Phi_j(y)dy = -\ddot{\alpha}(t)\int_0^l \rho(y)\Phi_j(y)dy \tag{27}$$

Now, substituting equations (7) and (9) into equation (4) and doing appropriate mathematical manipulation, one obtain that β

$$\beta_j = -\frac{1}{M_t}\int_0^l \rho(y)\Phi_j(y)dy \tag{28}$$

Substituting equations (8) and (28) into equation (27), for $i = j$

$$\ddot{q}_i(t) + \omega_i^2 q_i(t) = F(t)\beta_i\,, \quad i = 1,2,\ldots,\infty. \tag{29}$$

Note that $q_i\ (t)$ can be obtained by integrating equation (27) for given values of ω_i and applied force $F\ (t)$. For given $\psi_i(l)$, β_i and $q_i(t)$, the beam deflection can be expressed as

$$u(y,t) = \sum_{i=1}^{\infty}\Phi_i(y)q_i(t) = \sum_{i=1}^{\infty}\left[\psi_i(y) - \beta_i\right]q_i(t) \tag{30}$$

Accordingly, the position of the cart can be expressed as

$$x(t) = \alpha(t) + \sum_{i=1}^{\infty}\beta_i q_i(t) \tag{31}$$

Now, the nonhomogeneous equations (8) and (29) can be transformed into a set of $n+1$ second-order ordinary differential equations of the form

$$\begin{pmatrix} M_t & 0 \\ 0 & I \end{pmatrix}\begin{pmatrix} \ddot{\alpha} \\ \ddot{q}_i \end{pmatrix} + \begin{pmatrix} 0 & 0 \\ 0 & K \end{pmatrix}\begin{pmatrix} \alpha \\ q_i \end{pmatrix} = \begin{pmatrix} 1 \\ \beta_i \end{pmatrix}F(t), \ i = 1,2,\ldots,n. \tag{32}$$

Where K represents an $n \times n$ stiffness matrix such that $K = diag\{\omega_i^2\}$. Equation (32) can be solved using the fourth order Runge-Kutta method for an arbitrary given forcing function $F(t)$.

4. DESIGN OF ACTIVE MODAL CONTROLLER

In this section, the design of an active optimal controller for the vibration suppressing of elastic cantilever beam mounted on a moving cart and carrying tip lumped mass is tackled. The elastic beam was already modeled in section 3 via the unconstrained modal analysis from which the transient response of the tip beam deflection can be obtained as per equation (29). To eliminate the need for sensor placement on the tip of the cantilever beam since most of the practical control implementations required that sensors and actuators be placed at certain accessible structural locations, Linear Quadratic Estimator (LQE) technique is used for estimating the vibration of any point on the span of the flexible cantilever beam mounted on a moving cart and carrying tip lumped mass and subjected to process and measurement noises. Linear-quadratic-Gaussian (LQG) control is a modern state-space technique for designing optimal dynamic regulators. It enables to trade off regulation performance and control effort. Also it takes into account process disturbances and measurement noises. Fig. 2 illustrates the schematic of the LQG approach. The main goal of this control scheme is to regulate the output y around zero. The plant is subjected to disturbances w and is driven by controls u. The regulator relies on the noisy measurements $\bar{y} = y + v$ to generate these controls. The plant states and measurement equations are expressed as

$$\dot{z} = Az + Bu + Bw, \quad y = Cz + Du + v \tag{33}$$

where A is the plant state matrix , B is the plant input matrix , C is the plant output matrix , D is the plant feed forward, and both w and v are modeled as white noise. The LQG regulator consists of an optimal state-feedback gain and a Kalman state estimator. The design of these two components is discussed hereafter with more details.

<u>Optimal state feedback gain:</u> In LQG controller, the regulation performance J is measured by a quadratic performance criterion of the form

$$J(u) = \int_0^\infty \left[z^T(t) Q\, z(t) + u^T R\, u(t) \right] \tag{34}$$

The weighting matrices Q and R define the trade-off between regulation performance (how fast goes to zero) and control effort. The first design step seeks a state-feedback law $u = -\overline{K}\, x$ that minimizes the cost function $J(u)$. The minimizing gain matrix $\overline{K}$ is obtained by solving the associated algebraic Riccati equation.

<u>Kalman Filter Estimator:</u> Kalman filter is an optimal recursive data processing algorithm. One aspect of this optimality is that the Kalman filter incorporates all information that can be provided to it such as knowledge of the system , measurement device dynamics ,statistical description of the system noises , measurement errors, and uncertainty in the dynamic model .Unlike certain data processing concepts , the Kalman filter doesn't require all previous data to be kept in storage and reprocessed every time , but a new measurement is taken each time .Fig. 3 depicts a typical situation in which a Kalman filter can be used advantageously . The input disturbances are included in the state space model by adding the noise input vector w to the exogenous input vector u. Moreover, to include measurement noise, the vector v is added to the output of the system. Such noise signals are usually

part of the actual mode of the system. Up to this end, the LQG regulator can be established by combining the Kalman filter and LQ-optimal gain *K* as shown in Fig. 4.

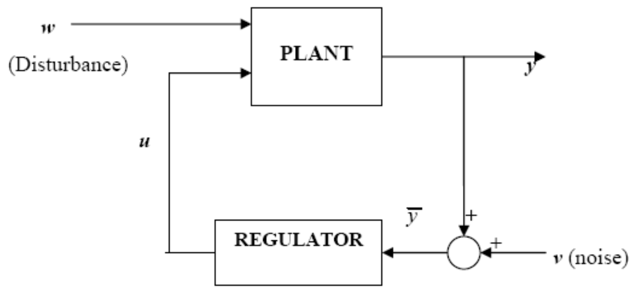

Fig. 2: Schematic of the proposed LQG approach.

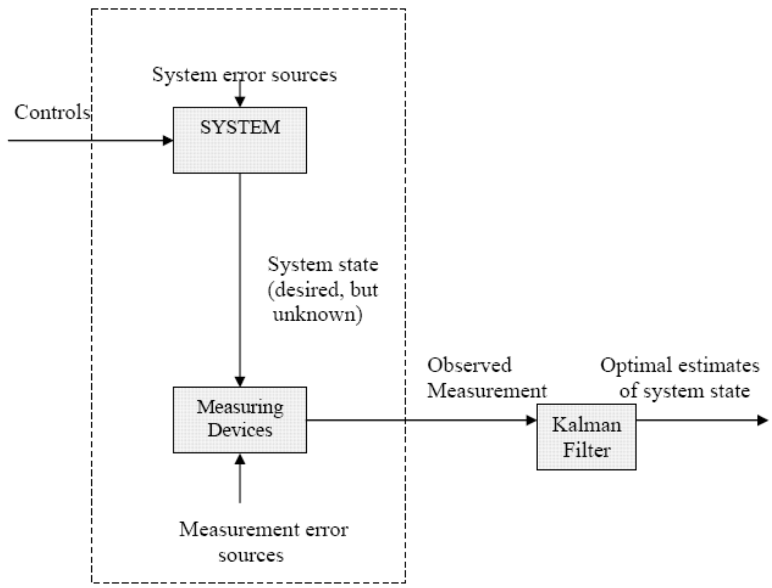

Fig. 3: Typical Kalman filter application.

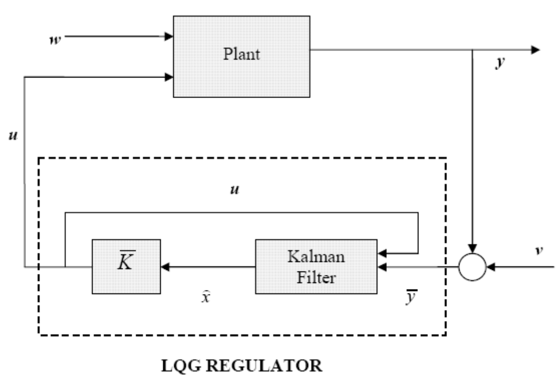

Fig. 4: Schematic flow chart for Linear Quadratic Guassian Regulator.

5. NUMERICAL SIMULATION

The main objective of the current numerical study is to examine both open and closed loop responses after implementing the developed LQG controller. The beam tip deflection was estimated using Kalman filter estimator, in the presence of process and measurement noises using Kalman filter estimator. Numerical values of the system parameters are selected as shown in table 1.

Table 1: System Parameters

Parameters	Value
Mass of cart, *M*	10.0 kg
Length of elastic beam, *L*	1.0 m
Mass per unit length of elastic beam, ρ_o	0.788 kg/m
Young's modulus of elastic beam, *E*	2.07×10^{-11} N/m^2
Area moment of inertia of elastic beam, *I*	5.208×10^{-11} m^4

5.1 Open-loop Response of the beam-mass-cart system

Numerical simulations were carried out to examine the open-loop response of the system, subjected to a periodic forcing function, such that $f(t) = 10\cos(10t)$. Equation (32) has been solved numerically, using ODE 45 solver within MATLAB® software, and numerical solutions were obtained by integrating the discretized form of the equations forward in time. The natural frequencies of the system have been obtained by solving the frequency equation presented in equation (25) utilizing Newton-Raphson method, for each mode of vibration. Table 2 show the obtained modal and natural frequencies for the first three modes of vibration, in addition to the corresponding values of the constants *C*, *D*, $\psi_i\,(l)$ and β_i which have been evaluated based on their definitions presented in the aforementioned modal analysis. Figures 5 show the time responses of both displacement and velocity at the tip of the beam for the first three modes of vibration when the system is subjected to the sinusoidal force. Referring to fig. 5, it was found that the most critical mode is the first one, as the applied sinusoidal force leads to large deflection of the elastic beam compared with the other modes of vibration. This finding is considered reasonable enough to design a controller to suppress the vibration for the first dominant mode. It is obvious that the vibration signal appears just like noise at high modes of vibration.

Table 2: The values of the modal and natural frequenc and associated modal the first three modes of vibration.

First Mode (i=1) (k =1.2267, ω_n=5.566 rad/s)				Second Mode (i=2) (k =4.03, ω_n=60.073 rad/s)				Third Mode (i=3) (k =7.132, ω_n=188.143 rad/s)			
C	*D*	$\psi_i(L)$	β_i	*C*	*D*	$\psi i\,(L)$	β_i	*C*	*D*	$\psi_i\,(L)$	β_i
-0.135	-0.082	0.871	-0.109	0.164	-0.006	0.244	-0.04	-0.1511	-0.003	0.166	-0.025

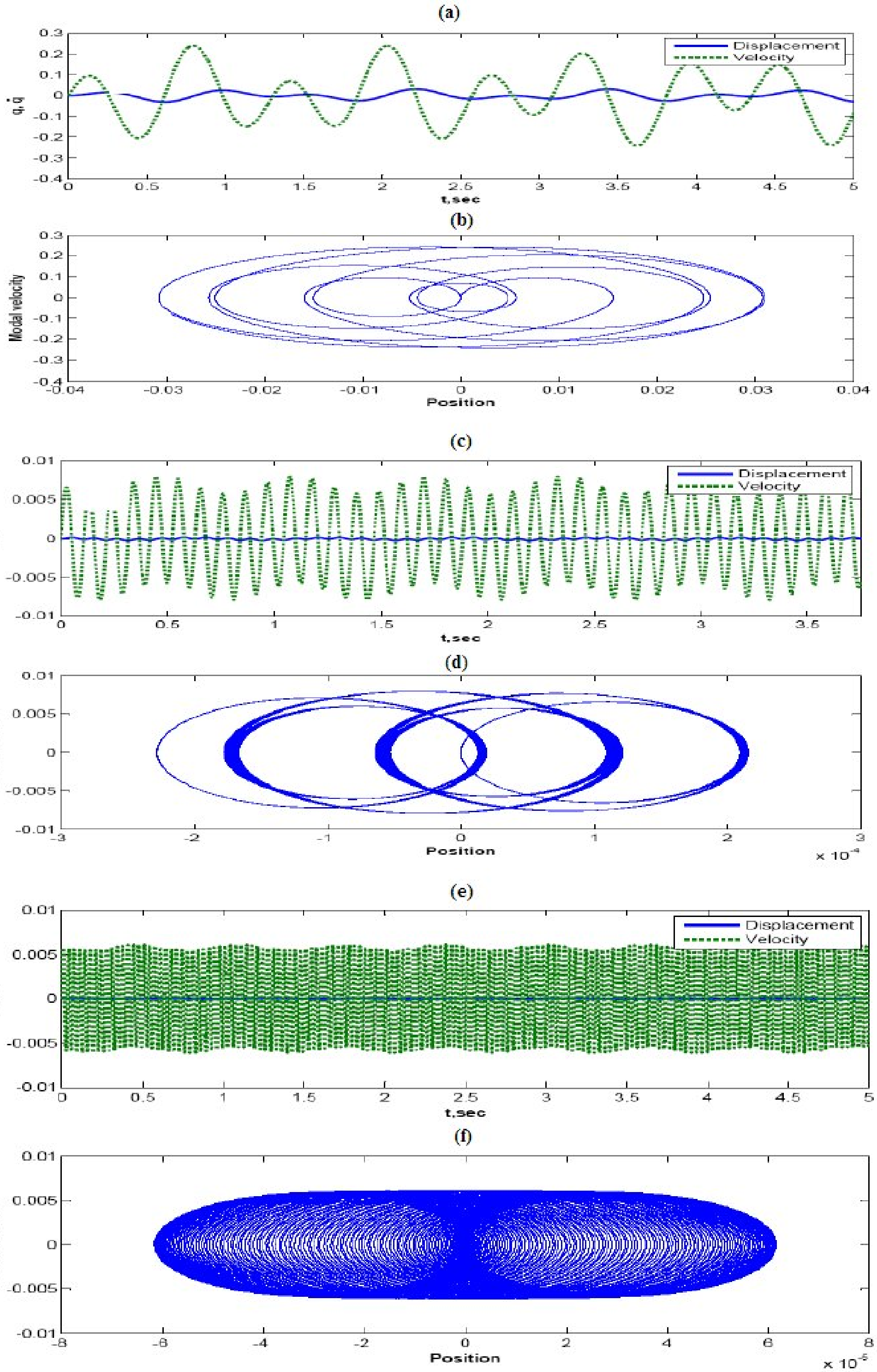

Fig. 5: (a) Open-loop response of the local beam deflection at the first mode of vibration when $f(t) = 10\cos(10t)$. (b) Corresponding phase plane plot. (c) Open-loop response of the local beam deflection at the 2nd mode of vibration (d) Corresponding phase plane plot. (e) Open-loop response of the local beam deflection at the 3rd mode of vibratio. (f) Corresponding phase plane plot.

The phase plane plot shows that there is one equilibrium point for the beam-mass-cart system where there is no excitation force and the expected shape of phase plane plot in that case is a center profile. On the other hand, the importance of the phase plane plot appears clearly in determining the qualitative behavior of the dynamic systems such as stability.

5.2 Estimated beam tip deflection in the presence of process and measurement noises using Kalman filter estimator.

In this part, Kalman filter is used to estimate the beam tip deflection in the presence of process disturbance w and noise measurements v. In order to illustrate the efficiency of the filtration process, the excitation force applied to the system is chosen to be similar to the selected force in the open loop analysis. The process disturbance signal w is selected to be a random force of magnitude of $\pm 2\,\mathrm{N}$. Matlab Simulink model has been developed to represent the Kalman filter estimator in order to predict the beam tip deflection in the presence of process and noise measurements. Kalman filter matrix was obtained using a simple Matlab algorithm, while the beam-mass-cart system has been defined in its state space representation. In order to demonstrate the capability of the proposed filtration scheme, the estimated beam tip deflection is compared with the corresponding value obtained via the unconstrained modal analysis. Fig. 6 shows the capability of the proposed estimator in producing fairly accurate tip deflection. Kalman filter was found as powerful tool to eliminate hysteresis obtained by process and measurement noises and to purify the output signal.

5.3 Closed-loop response using LQG optimal controller

In order to illustrate the regulator performance, both open and closed responses of the deflection at the tip of the beam subjected to the periodic functions were compared as shown in figures 7 and 8 for different weighting matrices. Referring to these figures, it was found that the linear quadratic regulator is considered as efficient tool to eliminate the vibrations and stabilize the system for various inputs. It is important to recognize that the dynamic matrix of the system shows that the system is conditionally stable since the roots are pure imaginary while the new eigenvalues for the system after using regulator are with negative real parts which assure stability for the system. By examining figures 7 and 8, we can conclude that the time required to achieve the steady state response can be controlled by by increasing the weight of (Q) matrix and/or decreasing the weight matrix (R) which has been used in LQ regulator .Fig. 8 shows a fast closed loop response which was obtained by decreasing the value of the weighting matrix (R). Generally if application requires fast decay of vibration, weighting matrix (Q) must be increased while (Q) matrix shall be decreased, and the opposite can be performed if reduction of the control effort is required.

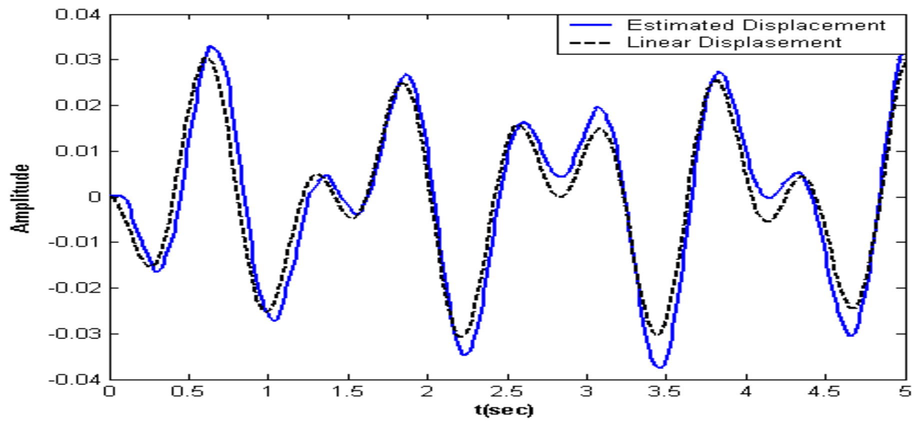

Fig. 6: Estimated beam tip deflection in presence of process and measurement noises using Kalman filter estimator versus deflection obtained using unconstrained modal analysis for the first mode of vibration.

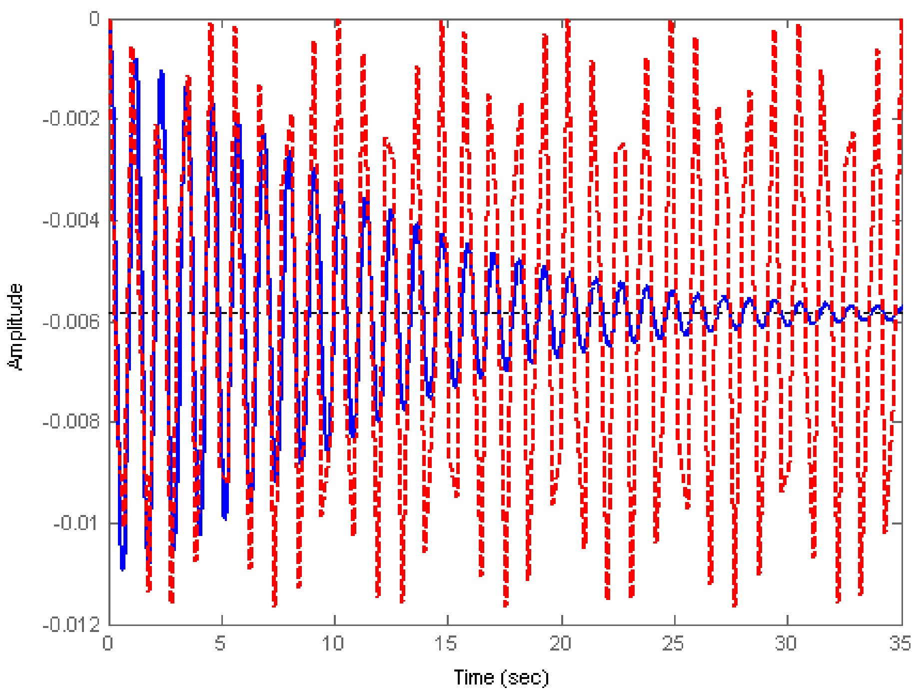

Fig. 7: Open loop versus closed loop (Regulated) responses for periodic input with weighting matrix (R=0.01).

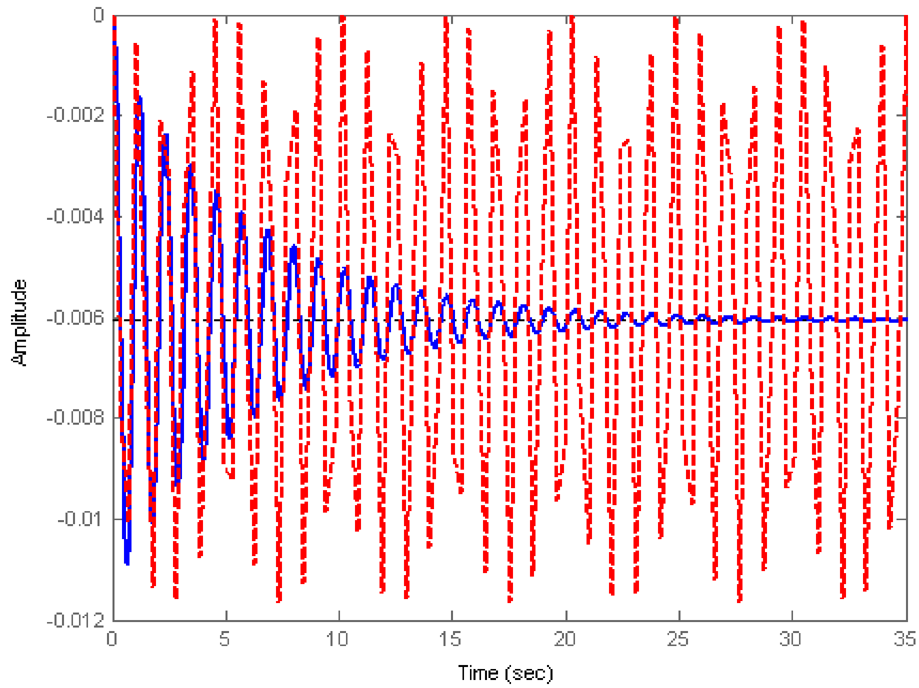

Fig. 8: Open loop versus closed loop (Regulated) responses for periodic input after with weighting matrix (R=0.001).

6. CONCLUSIONS

In the present work, a Bernoulli – Euler beam fixed on a moving cart and carrying lumped tip mass was considered and the equations of motion which describe the global motion as well as the vibration motion were derived by means of the extended Hamilton's principle .A unified frequency equation was obtained and the roots of the frequency equation were found for the first three modes of vibrations. Exact and assumed-mode solutions were obtained by the unconstrained modal analysis for the beam-mass-cart system which emphases the importance of unconstrained modal analysis in studying the effect of the axial movement of the cart and achieving accurate mode shapes. In order to eliminate the need for sensor placement on the tip of the cantilever beam ,since most of the practical control implementations required that sensors and actuators be placed at certain accessible structural locations ,a new approach based on the Linear Quadratic Estimator (LQE) technique for estimating the vibration of any point on the span of the flexible cantilever beam mounted on a moving cart and carrying tip lumped mass and subject to process and measurement noise has been developed. Numerical simulation results demonstrated the capability of the proposed estimator in producing fairly accurate tip deflection. The analytical design of an active optimal scheme for vibration suppression was employed via the Linear Quadratic Regulator (LQR) to obtain the output feedback control gain. Closed-loop responses obtained by the proposed technique were compared to the open-loop responses generated by the unconstrained analysis and the results showed good vibration suppression.

ACKNOWLEDGEMENTS

The author is grateful for the support provided by King Fahd University of Petroleum and Minerals.

REFERENCES

1. **Bhat, R. and Wanger H., (1976),** "Natural frequencies of a uniform cantilever with a tip mass slender in the axial direction", Journal of Sound and Vibration 45, 304-307.
2. **To, W. S., (1982),** "Vibration of a cantilever beam with a base excitation and tip mass', Journal of Sound and Vibration 83, 445-460.
3. **Park, S. D., Chung, W. K., Youm, Y. and Lee, J. W., (1998**), "Analysis of the motion of a cart with an inverted flexible beam and a concentrated tip mass", Proceedings of Korean Automatic Control Conference (KACC), 367-372.
4. **Park, S. D., Chung, W. K., Youm, Y. and Lee J. W., (2000),** 'Natural frequencies and open-loop responses of an elastic beam fixed on a moving cart and carrying an intermediate lumped mass", Journal of Sound and Vibration 230**,** 591-615.
5. **Khulief, Y. A., (2000),** "Vibration suppression in rotating beams using active modal control", Journal of Sound and Vibration 242**,** 681-699.
6. **Zimmerman, C. and Cudeney H. H., (1989),** "Practical implementation issues for active control of large flexible structures", Journal of Vibration, Acoustics, Stress, and Reliability in Design 111,283-289 .
7. **Yousifi-Koma and Voukovich G., (2000),** "Vibration suppression of flexible beams with ponded piezo transducers using wave-absorbing controllers", Journal of Guidance, Control, and Dynamics 23, 347-354.
8. **Mallory W. and Miller D., (2000),** "Decentralized state estimation for flexible space structures", Journal of Guidance, Control, and Dynamics 23, 665-672.
9. **Lee Y. and Elliott S., (2001),** "Active position control of flexible smart beam using internal model control", Journal of Sound and Vibration 242, 767-791.
10. **El-Sinawi A. and Hamdan M. (2003),** "Optimal vibration estimation of a non-linear flexible beam mounted on a rotating compliant hub", Journal of Sound and Vibration 259, 857-872.